European Polymer Journal 45 (2009) 2234–2248

Contents lists available at ScienceDirect

European Polymer Journal

journal homepage: www.elsevier.com/locate/europolj

Electroactive aromatic polyamides and polyimides with adamantylphenoxy-substituted triphenylamine units

Sheng-Huei Hsiao [a,*], Guey-Sheng Liou [b], Yi-Chun Kung [c], Hung-Yin Pan [c], Chen-Hua Kuo [c]

[a] Department of Chemical Engineering and Biotechnology, National Taipei University of Technology, Taipei 10608, Taiwan
[b] Institute of Polymer Science and Engineering, National Taiwan University, Taipei 10617, Taiwan
[c] Department of Chemical Engineering, Tatung University, Taipei 10452, Taiwan

ARTICLE INFO

Article history:
Received 21 March 2009
Received in revised form 8 May 2009
Accepted 13 May 2009
Available online 18 May 2009

Keywords:
Polyamides
Polyimides
Electrochemistry
Electrochromism

ABSTRACT

A new triphenylamine-containing aromatic diamine monomer, 4-[4-(1-adamantyl)phenoxy]-4′,4″-diaminotriphenylamine, was synthesized from cesium fluoride-mediated *N*,*N*-diarylation of 4-(1-adamantyl)-4′-aminodiphenyl ether with 4-fluoronitrobenzene and subsequent reduction of the resultant dinitro compound. Novel electroactive aromatic polyamides and polyimides with adamantylphenoxy-substituted triphenylamine moieties were prepared from the newly synthesized diamine monomer with aromatic dicarboxylic acids and tetracarboxylic dianhydrides, respectively. All the resulting polymers were amorphous and most of them were readily soluble in polar solvents such as *N*-methyl-2-pyrrolidone (NMP) and *N*,*N*-dimethylacetamide (DMAc) and could be solution-cast into transparent and strong films with good mechanical properties. These polymers exhibited glass-transition temperatures between 254 and 310 °C, and they were fairly stable up to a temperature above 450 °C for the polyamides and above 500 °C for the polyimides. These polymers exhibited strong UV–vis absorption maxima at 293–346 nm in solution, and the photoluminescence spectra of polyamides showed maximum bands around 408–452 nm in the blue region. Cyclic voltammograms of the polyamide and polyimide films on an indium–tin oxide (ITO)-coated glass substrate exhibited one pair of reversible redox couples at half-wave oxidation potentials ($E_{1/2}$) around 0.83–0.86 V and 1.12–1.13 V, respectively, versus Ag/AgCl in an acetonitrile solution. All the polymer films revealed good electrochemical and electrochromic stability by repeatedly switching electrode voltages between 0.0 V and 1.1–1.4 V, with coloration change from the pale yellowish neutral state to the green or blue oxidized state.

1. Introduction

Because of the easy oxidizability of the nitrogen center and the ability to transport positive charge centers via the radical cation species, triarylamine derivatives are known hole-transport materials that played important roles in organic light emitting devices as well as in other organic electronics [1,2]. The structural unit of triarylamine responsible for the hole transporting property can be covalently bonded with one another or can be attached to a polymer backbone through substituents to obtain a wide variety of low molecular weight compounds as well as polymers [3]. Several studies have reported improvements in hole injecting and transporting properties when a triarylamine structure is incorporated into the main chain of light-emitting polymers or as an end-capper or a side chain [4–12].

Aromatic polyamides and polyimides are well-known high-performance polymers that have excellent thermal, mechanical and electrical properties as well as outstanding chemical resistance [13–16]. However, most of them have high melting or softening temperature and are insoluble in most of organic solvents because of the rigidity of the backbone and strong intermolecular interactions. These proper-

* Corresponding author. Tel.: +886 2 27712171x2548; fax: +886 2 27317117.
E-mail address: shhsiao@ntut.edu.tw (S.-H. Hsiao).

0014-3057/$ - see front matter © 2009 Elsevier Ltd. All rights reserved.
doi:10.1016/j.eurpolymj.2009.05.017

ties make them generally intractable or difficult to process; thus, their applications are restricted in some fields. To overcome these limitations, many efforts have been made to improve the processing characteristics of these intractable polymers while other advantageous properties are retained [17–20]. Different structural modifications of the polymer backbone have been studied to reduce the chain–chain interaction, e.g., the incorporation of bulky, packing-disruptive moieties which hinder the chain packing but do not markedly affect the glass transition temperature [21–28]. It has been demonstrated that aromatic polyamides and polyimides containing bulky, propeller-shaped triphenylamine (TPA) unit were amorphous, had excellent or enhanced solubility in organic solvents, and exhibited high thermal stability [29–36]. In recent years, we have reported that many TPA-based polyamides and polyimides show interesting electrochromic properties and some of them are very stable toward redox cycling, which makes them potential candidates for commercial device applications [37–43]. Therefore, the introduction of TPA unit into aromatic polyamide and polyimide backbones would be expected to be a potential structural approach for not only increasing solubility without sacrificing high thermal stability but also allowing them to be used as potential hole-transporting or electrochromic materials.

Adamantane (tricyclo[3.3.1.1^{3,7}]decane) is a highly symmetrical tricyclic hydrocarbon, which consists of fused chair-form cyclohexane rings [44]. The unique structure of this substance is reflected in highly unusual physical and chemical properties such as thermal and oxidation stabilities, low surface energy, and high hydrophobicity. The incorporation of adamantyl groups into aromatic polyamides and polyimides has been reported to improve solubility or dielectric properties while retaining high thermal stability and glass-transition temperatures [45–53]. The improvement of solubility and thermal properties of adamantyl containing polymers results from the rigidity and the bulkiness of the adamantyl moiety, which greatly reduces the chain mobility and inhibits chain packing. As part of our continuing efforts in the structural modification of the TPA-containing high-performance polymers, this study deals with the synthesis and properties of new TPA-based polyamides and polyimides with bulky pendent adamantylphenoxy groups from a newly synthesized diamine monomer, 4-[4-(1-adamantyl)phenoxy]-4′,4″-diaminotriphenylamine, and various aromatic dicarboxylic acids and tetracarboxylic dianhydrides. The prepared polyamides and polyimides were expected to have increased organo-solubility because of the presence of three-dimensional TPA unit and bulky adamantylphenoxy pendants. These polymers were also expected to exhibit more stable redox, electrochromic, and hole-transport properties because the *para*-positions of the pendent phenyl groups are blocked with the adamantylphenoxy group.

2. Experimental

2.1. Materials

1-Bromoadamantane (Acros), phenol, *p*-chloronitrobenzene (Acros), potassium carbonate (K_2CO_3) (Fluka), cesium fluoride (CsF) (Acros), palladium on charcoal (Pd/C) (Fluka), *p*-fluoronitrobenzene (Acros), triphenyl phosphite (TPP) (Acros), and hydrazine monohydrate (TCI) were used without further purification. *N*,*N*-Dimethylacetamide (DMAc) (Tedia), *N*,*N*-dimethylformamide (DMF) (Tedia), pyridine (Py) (Wako) and *N*-methyl-2-pyrrolidone (NMP) (Tedia) were dried over calcium hydride for 24 h, distilled under reduced pressure, and stored over 4 Å molecular sieves in a sealed bottle. The commercially available aromatic dicarboxylic acids that included terephthalic acid (**6a**) (Wako), isophthalic acid (**6b**) (Fluka), 4,4′-biphenyldicarboxylic acid (**6c**) (TCI), 1,4-naphthalenedicarboxylic acid (**6d**) (Wako), 2,6-naphthalenedicarboxylic acid (**6e**) (TCI), 4,4′-dicarboxydiphenyl ether (**6f**) (TCI), 4,4′-dicarboxydiphenyl sulfone (**6g**) (New Japan Chemical Co.), and 2,2-bis(4-carboxyphenyl)hexafluoropropane (**6h**) (Chriskev) were used as received. Commercially obtained calcium chloride was dried under vacuum at 180 °C for 8 h prior to use. Commercially available aromatic tetracarboxylic dianhydrides such as pyromellitic dianhydride (PMDA; **8a**, from Aldrich) and 3,3′,4,4′-benzophenonetetracarboxylic dianhydride (BTDA; **8c**, from Aldrich) were purified by recrystallization from acetic anhydride. 3,3′,4,4′-Biphenyltetracarboxylic dianhydride (BPDA; **8b**, from Oxychem), 4,4′-oxydiphthalic anhydride (ODPA; **8d**, from Oxychem), 3,3′,4,4′-diphenylsulfonetetracarboxylic dianhydride (DSDA; **8e**, from New Japan Chemical Co.), and 2,2-bis(3,4-dicarboxyphenyl)hexafluoropropane dianhydride (6FDA; **8f**, from Hoechst Celanese) were heated at 250 °C *in vacuo* for 3 h before use. Tetrabutylammonium perchlorate (TBAP) (TCI) was recrystallized twice by ethyl acetate under nitrogen atmosphere and then dried *in vacuo* prior to use. All other reagents were used as received from commercial sources.

2.2. Monomer synthesis

2.2.1. 4-(1-Adamantyl)phenol (*1*)

A 500 mL round-bottom flask was charged with 32.3 g (0.15 mol) of 1-bromoadamantane and 141.2 g (1.5 mol) of phenol. The flask was fitted with a reflux condenser and one outlet leading to a beaker with a NaOH solution to trap the HBr evolved in the reaction. The reaction mixture was stirred at 80 °C for 10 h. The excess phenol was then removed by stirring the product in 500 mL portions of hot water three times. The yield of the crude product was 33 g (96%). The crude product was further purified by recrystallization from a methanol/water mixture as off-white needles with a mp of 177–178 °C by DSC at scanning rate 2 °C/min (lit. [54] 181–183 °C). IR (KBr, cm^{-1}): 3222 (O–H str), 1214 (C–O str). ^{1}H NMR (500 MHz, DMSO-d_6, δ, ppm): 7.12 (d, J = 8.6 Hz, 2H, H_d), 6.70 (d, J = 8.6 Hz, 2H, H_e), 2.20 (broad singlet (br s), 3H, H_b), 1.79 (br s, 6H, H_c), 1.73 (two overlapped AB doublets, 6H, H_a). ^{13}C NMR (125 MHz, DMSO-d_6, δ, ppm): 155.2 (C^8), 141.8 (C^5), 125.8 (C^6), 115.1 (C^7), 43.3 (C^3), 36.6 (C^1), 35.3 (C^4), 28.8 (C^2).

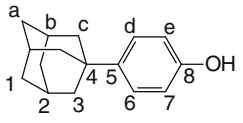

*2.2.2. 4-(1-Adamantyl)-4′-nitrodiphenyl ether (**2**)*

4-(1-Adamantyl)phenol (22.8 g, 0.10 mol), *p*-chloronitrobenzene (15.8 g, 0.10 mol), and potassium carbonate (14.0 g, 0.10 mol) were dissolved/suspended in 120 mL DMF in a 500 mL round-bottom flask. The reaction mixture was heated to 150 °C and held at that temperature for 12 h. After cooling to room temperature, the mixture was poured into 200 mL/200 mL water/methanol. The yellow precipitate was filtered, washed with water, and dried. The yield of the crude product was 34 g (97%). The crude product was purified by recrystallization from a DMF/ethanol mixture as pale-yellow needles; mp = 171–173 °C. IR (KBr, cm^{-1}): 1584, 1367 ($-NO_2$ str).

*2.2.3. 4-(1-Adamantyl)-4′-aminodiphenyl ether (**3**)*

In a 500 mL round-bottom flask, fitted with a magnetic stir bar and a reflux condenser, were placed compound **2** (30 g, 0.086 mol), ethanol 200 mL, 10% Pd/C (0.2 g), and hydrazine monohydrate 15 mL. The reaction mixture was slowly heated to 90 °C and stirred for 4 h. The resultant clear, darkened solution was filtered while hot to remove Pd/C. Upon cooling, the product crystallized as off-white needles from the filtrate; yield 22.4 g (82%); mp = 118–119 °C (by DSC, 2 °C/min). IR (KBr, cm^{-1}): 3421, 3343, 3223 ($-NH_2$ str). ^{1}H NMR (500 MHz, DMSO-d_6, δ, ppm): 7.22 (d, J = 8.5 Hz, 2H, H_d), 6.78 (d, J = 8.5 Hz, 2H, H_e), 6.75 (d, J = 8.5 Hz, 2H, H_f), 6.64 (d, J = 8.5 Hz, 2H, H_g), 4.93 (s, 2H, $-NH_2$), 2.00 (br s, 3H, H_b), 1.79 (br s, 6H, H_c), 1.69 (two overlapped AB doublets, 6H, H_a). ^{13}C NMR (125 MHz, DMSO-d_6, δ, ppm): 156.9 (C^8), 146.4 (C^9), 145.4 (C^{12}), 144.7 (C^5), 126.1 (C^6), 121.0 (C^{10}), 116.4 (C^{11}), 115.4 (C^7) 43.1 (C^3), 36.5 (C^1), 35.5 (C^4), 28.7 (C^2).

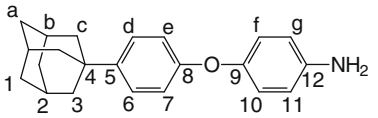

*2.2.4. 4-[4-(1-Adamantyl)phenoxy]-4′,4″-dinitrotriphenylamine (**4**)*

A mixture of the aromatic ether-amine **3** (16.0 g, 0.05 mol), *p*-fluoronitrobenzene (14.1 g, 0.1 mol), cesium fluoride (CsF) (15.2 g, 0.1 mol), and DMSO (100 mL) was heated and stirred at 120 °C for 10 h. The reaction mixture was cooled and poured into a water/methanol (500 mL/500 mL). The yellow precipitate was filtered, washed with water, and dried. The yield of the crude product was 26.7 g (95%). The crude product was purified by recrystallization from DMF/methanol as yellow crystals; mp = 248–251 °C (by DSC, 2 °C/min). IR (KBr, cm^{-1}): 1579, 1340 ($-NO_2$ str).

*2.2.5. 4-[4-(1-Adamantyl)phenoxy]-4′,4″-diaminotriphenylamine (**5**)*

A mixture of dinitro compound **4** 22.5 g (0.04 mol), ethanol 200 mL, 10% Pd/C 0.2 g, and hydrazine monohydrate 16 mL was heated at 80 °C for 2 h. The resultant clear, darkened solution was filtered while hot to remove Pd/C. The filtrate was stored in a refrigerator, and the product gradually precipitated as gray crystals; yield 15 g (75%); mp = 225–228 °C (by DSC, 2 °C/min). IR (KBr, cm^{-1}): 3435, 3350 ($-NH_2$). ^{1}H NMR (500 MHz, DMSO-d_6, δ, ppm) (for the peak assignments, see Fig. 2a): 7.20 (d, J = 8.5 Hz, 2H, H_d), 6.80 (d, J = 8.5 Hz, 2H, H_e), 6.79 (d, J = 8.5 Hz, 4H, H_h), 6.73 (d, J = 9.0 Hz, 2H, H_f), 6.66 (d, J = 9.0 Hz, 2H, H_g), 6.57 (d, J = 8.5 Hz, 4H, H_i), 1.98 (br. s., 3H, H_b), 1.77 (br s, 6H, H_c), 1.69 (two overlapped AB doublets, 6H, H_a). ^{13}C NMR (125 MHz, DMSO-d_6, δ, ppm) (for the peak assignments, see Fig. 2b): 156.0 (C^8), 148.5 (C^9), 146.0 (C^{12}), 145.3 (C^{16}), 145.2 (C^5), 137.1 (C^{13}), 126.9 (C^{14}), 126.2 (C^6), 120.2 (C^{10}), 119.3 (C^{11}), 117.1 (C^7), 115.4 (C^{15}), 43.1 (C^3), 36.5 (C^1), 35.5 (C^4), 28.6 (C^2). Anal. Calcd for $C_{34}H_{35}N_3O$ (501.67): C, 81.40%; H, 7.03%; N, 8.38%. Found: C, 81.31%; H, 7.02%; N, 8.29%.

2.3. Polymer synthesis

2.3.1. Synthesis of polyamides

The synthesis of polyamide **7a** is used as an example to illustrate the general synthetic route used to produce the polyamides. A 50 mL round-bottom flask equipped with a magnetic stirrer was charged with 0.5017 g (1 mmol) of diamine monomer **5**, 0.1661 g (1 mmol) of terephthalic acid (**6a**), 1 mL of TPP, 2 mL of NMP, 0.5 mL of pyridine, and 0.2 g of calcium chloride ($CaCl_2$). The reaction mixture was heated with stirring at 110 °C for 3 h. The resultant solution was poured slowly into 200 mL of methanol. The precipitate was washed thoroughly with methanol and hot water and then collected by filtration. The inherent viscosity of the polymer **7a** was 1.46 dL/g, measured at a concentration of 0.5 g/dL in DMAc containing 5-wt.% LiCl at 30 °C. IR (film, cm^{-1}): 3290 (N–H str), 1648 (C=O str), 2846, 2902 (adamantyl C–H str).

2.3.2. Synthesis of polyimides

The polyimides were synthesized from various commercial dianhydrides and diamine **5** via a two-step method. The synthesis of polyimide **10f** is used as an example to illustrate the general synthetic route used to produce the polyimides. To a solution of 0.7956 g (1.59 mmol) of diamine **5** in 14.2 mL of CaH_2-dried DMAc, 0.7044 g (1.59 mmol) of 6FDA was added in one portion. The mixture was stirred at ambient temperature for about 12 h to afford a highly viscous poly(amic acid) solution. The inherent viscosity of the resulting poly(amic acid) **9f** was 1.14 dL/g, measured in DMAc at a concentration of 0.5 g/dL at 30 °C. The poly(amic acid) was converted into polyimide using either a thermal or chemical imidization process.

For the thermal imidization method, about 7 g of the poly(amic acid) solution was transferred into a 9-cm glass Petri dish, which was baked at 90 °C for the removal of the casting solvent. The semi-dried poly(amic acid) film was further dried and converted to the polyimide by sequential heating at 150 °C for 30 min, 200 °C for 30 min, and 250 °C for 1 h. The IR spectrum of **10f** film exhibited characteristic imide absorption bands at 1780 cm^{-1} (asymmetrical C=O stretch) and 1734 cm^{-1} (symmetrical C=O stretch). ^{1}H NMR (500 MHz, $CDCl_3$, δ, ppm) (for the proton assignments, see Fig. 6): 1.77 (two overlapped AB doublets, 6H, H_a), 1.91 (br s, 6H, H_c), 2.1 (br s, 3H, H_b), 6.98–7.01 (t, 4H, $H_e + H_g$), 7.18 (d, 2H, H_f), 7.21 (d, 4H, H_h), 7.30 (d,

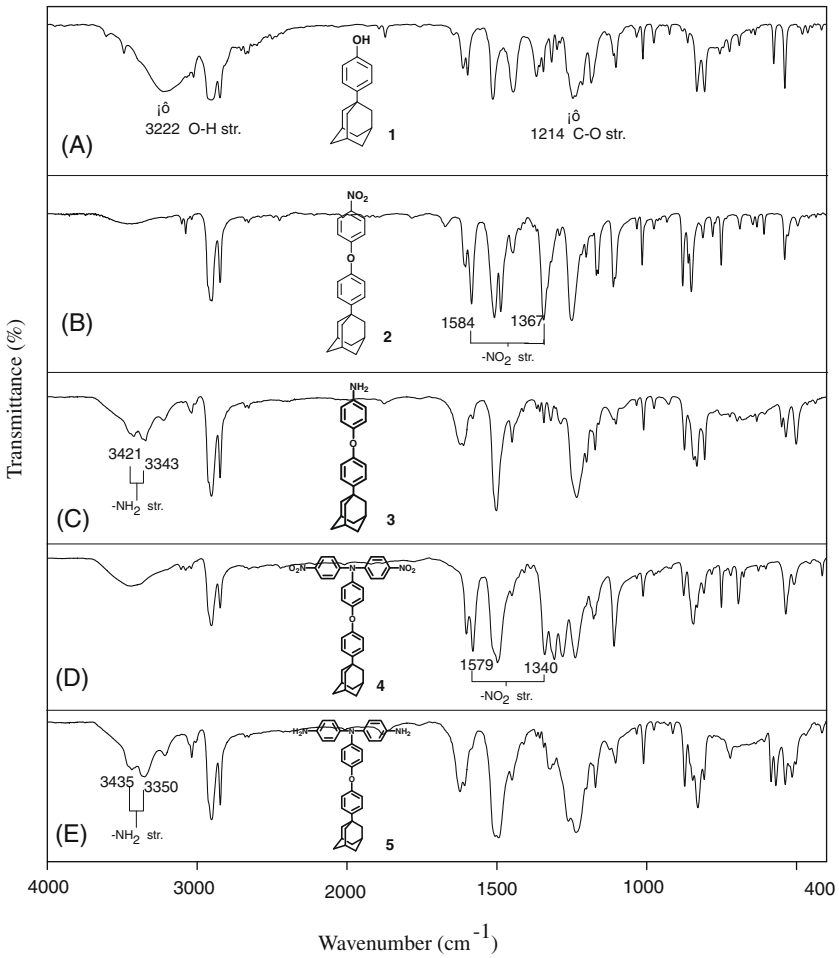

Fig. 1. IR spectra of the synthesized compounds **1**–**5**.

4H, H_i), 7.34 (d, 2H, H_d), 7.86 (d, 2H, H_k), 7.96 (s, 2H, H_l), 8.04 (d, 2H, H_j). For the tensile testing and thermal analyses, the polyimide film samples were further heated at 300 °C for 1 h.

For the chemical imidization method, 4 mL of acetic anhydride and 2 mL of pyridine were added to the remaining poly(amic acid) solution and the mixture was heated at 100 °C for 1 h to effect a complete imidization. The resultant solution of the polymer was poured slowly into 250 mL methanol giving rise to a yellow-coloring fibrous precipitate, which was washed thoroughly with methanol and hot water, collected by filtration, and dried. A polymer solution was made by the dissolution of about 0.5 g of the polyimide sample in 10 mL of hot DMAc. The homogeneous solution was poured into a 9-cm glass Petri dish, which was placed in a 90 °C oven overnight for the slow release of the solvent, and then the amber-coloring and transparent film was stripped off the glass substrate and further dried in vacuum at 160 °C for 6 h.

2.4. Preparation of the polyamide films

A polymer solution was made by the dissolution of about 0.7 g of the polyamide sample in 10 mL of hot DMAc. The homogeneous solution was poured into a 7-cm glass Petri dish, which was placed in a 90 °C oven overnight for the slow release of the solvent, and then the film was stripped off from the glass substrate and further dried in vacuum at 160 °C for 6 h. The obtained films were about 0.09 mm thick and were used for X-ray diffraction measurements, tensile tests, solubility tests, and thermal analyses.

2.5. Measurements

Elemental analyses were run in a HERAEUS VarioEL-III elemental analyzer. ^{1}H and ^{13}C NMR spectra were measured on a Bruker Avance 500 FT-NMR system with tetramethylsilane as an internal standard. Infrared (IR) spectra were recorded on a Horiba FT-720 FT-IR spectrometer. The inherent viscosities were determined with a Cannon–Fenske viscometer at 30 °C. Differential scanning calorimetry (DSC) was performed on a Perkin–Elmer Pyris 1 DSC at a scan rate of 20 °C/min in flowing nitrogen. Thermomechanical analysis (TMA) was determined with a Perkin–Elmer TMA 7 instrument. The TMA experiments were carried out from 50 to 350 °C at a scan rate of 10 °C/min with a penetration probe 1.0 mm in diameter under an applied constant load of

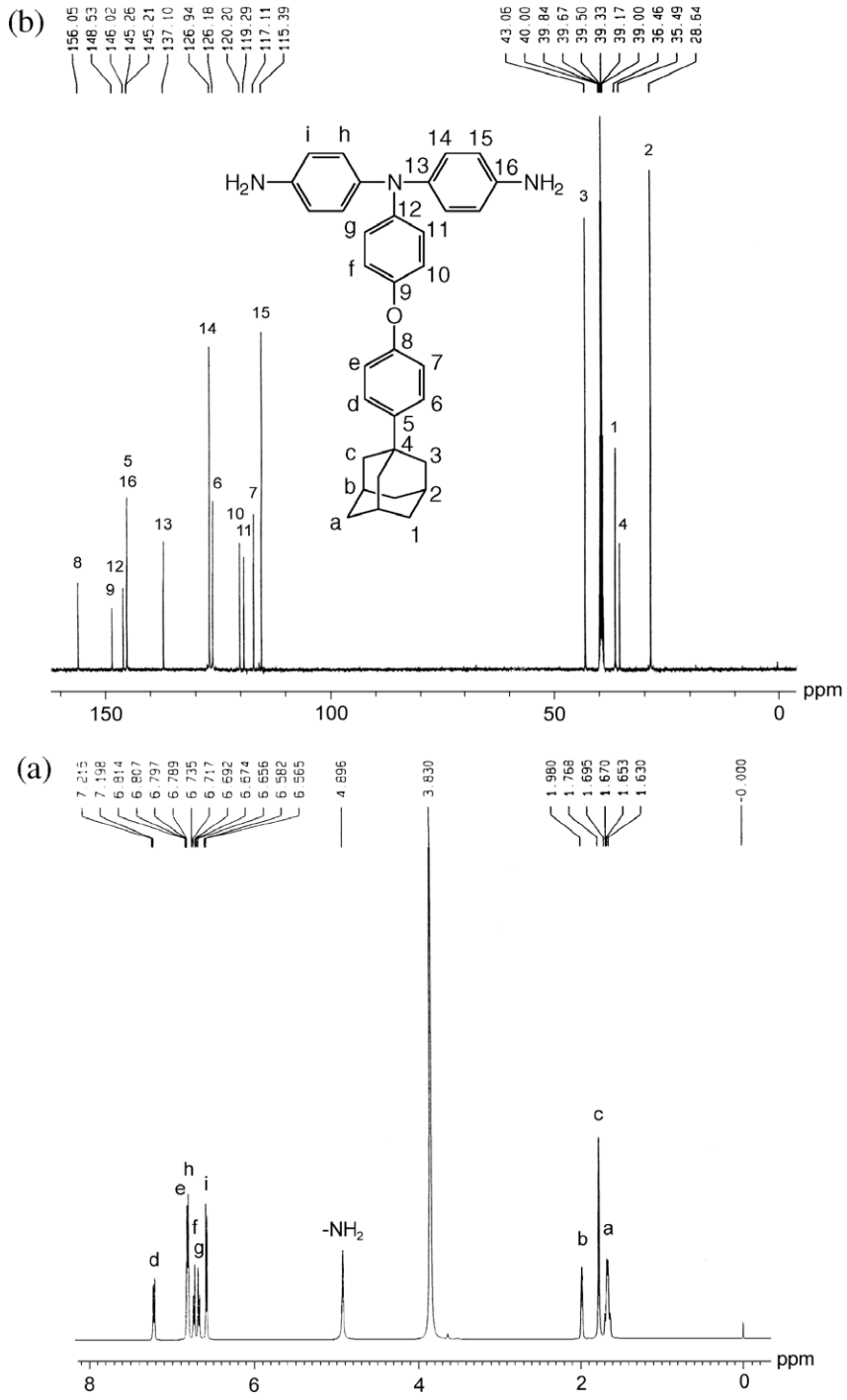

Fig. 2. (a) ^{1}H NMR and (b) ^{13}C NMR spectra of diamine monomer **5** in DMSO-d_6.

10 mN. Softening temperatures (T_s) were taken as the onset temperatures of probe displacement on the TMA traces. Thermogravimetric analysis (TGA) was performed with a Perkin–Elmer Pyris 1 TGA. Experiments were carried out on approximately 4–6 mg of samples heated in flowing nitrogen or air (flow rate = 40 cm^3/min) at heating rate of 20 °C/min. Wide-angle X-ray diffraction (WAXD) measurements were performed at room temperature (about 25 °C) on a Shimadzu XRD-6000 X-ray diffractometer with a graphite monochromator, using nickel-filtered Cu Kα radiation (λ = 1.5418 Å, operating at 40 kV and 30 mA). The scanning rate was 2°/min over a range of 2θ = 10–40°. A universal tester LLOYD LRX with a load cell 5 kg was used to study the stress–strain behavior of the samples. A gauge

length of 2 cm and a crosshead speed of 5 mm/min were used for this study. Measurements were performed at room temperature with film specimens (0.5 cm width, 6 cm length), and an average of at least three replicates was used. Electrochemistry was performed with a CH Instruments 600C electrochemical analyzer. Voltammograms are presented with the positive potential pointing to the left and with increasing anodic currents pointing downwards. Ultraviolet–visible (UV–vis) spectra of the polymer films were recorded on a Jasco UV–vis V530 spectrometer. Cyclic voltammetry was conducted with the use of a three-electrode cell in which ITO (polymer films area about 0.8 cm × 1.25 cm) was used as a working electrode. A platinum wire was used as an auxiliary electrode. All cell potentials were taken with the use of a homemade Ag/AgCl, KCl (sat.) reference electrode. Ferrocene was used as an external reference calibration (+0.48 V vs. Ag/AgCl). Spectroelectrochemistry analyses were carried out with an electrolytic cell, which was composed of a 1 cm cuvette, ITO as a working electrode, a platinum wire as an auxiliary electrode, and a Ag/AgCl reference electrode. Absorption spectra in the spectroelectrochemical experiments were measured with an Agilent 8453 UV–vis spectrophotometer. Photoluminescence (PL) spectra were measured with a VARIAN Cary Eclipse fluorescence spectrophotometer.

3. Results and discussion

3.1. Monomer synthesis

The TPA-based diamine monomer with a bulky adamantylphenoxy group, 4-[4-(1-adamantyl)phenoxy]-4′,4″-diaminotriphenylamine (**5**), was prepared starting from 1-bromoadamantane and phenol by a five-step reaction

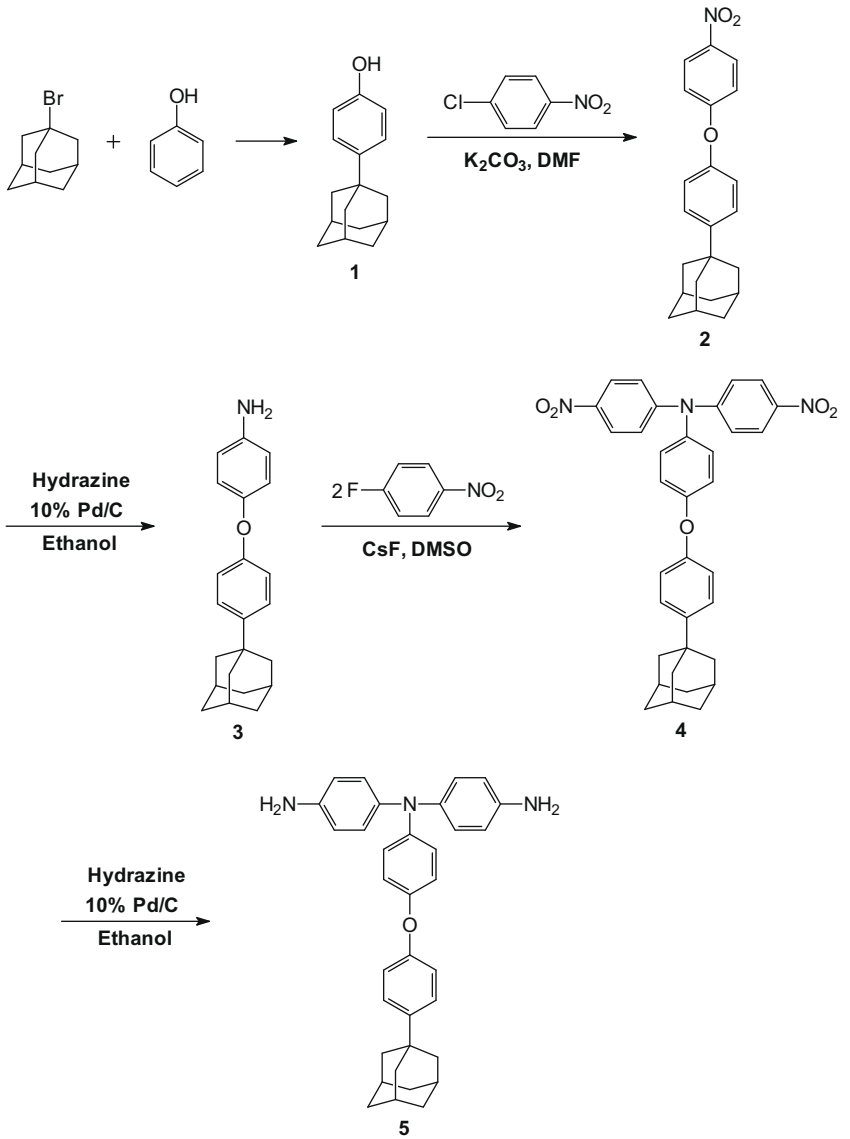

Scheme 1. Synthetic route to the target diamine monomer (**5**).

sequence, as outlined in Scheme 1. First, 4-(1-adamantyl)phenol (**1**) was synthesized by alkylation of phenol with 1-bromoadamantane according to a reported method [54]. Then, nucleophilic chlorodisplacement of *p*-chloronitrobenzene with the phenolate of **1** gave 4-(1-adamantyl)-4′-nitrodiphenyl ether (**2**), which was subsequently reduced to 4-(1-adamantyl)-4′-aminodiphenyl ether (**3**) by means of Pd/C and hydrazine. The target diamine monomer **5** was synthesized by double *N*-arylation reactions of **3** with two equivalent amount of *p*-fluoronitrobenzene in the presence of cesium fluoride, followed by hydrazine Pd/C-catalyzed reduction of the intermediate dinitro compound **4**. Elemental analysis, FT-IR, and ^{1}H and ^{13}C NMR spectroscopic techniques were used to identify the structures of the synthesized compounds. Fig. 1 shows the FT-IR spectra of all the synthesized compounds (**1**–**5**). The nitro groups of compounds **2** and **4** gave two characteristic bands at around 1580 and 1340–1370 cm^{-1} ($-NO_2$ asymmetric and symmetric stretching). After reduction, the characteristic absorptions of the nitro group disappeared and the amino group showed the typical N–H stretching absorption pair in the region of 3300–3500 cm^{-1}. Fig. 2 illustrates the ^{1}H and ^{13}C NMR spectra of the diamine monomer **5**. Assignments of each carbon and proton were assisted by the two-dimensional (2-D) COSY NMR spectra shown in Figs. 3 and 4, and these spectra agreed well with the proposed molecular structure of **5**. The ^{1}H NMR spectra confirm that the nitro groups have been completely transformed into amino groups by the high-field shift of the aromatic protons and by the resonance signals at around 4.9 ppm correspond to the amino protons.

3.2. Polymer synthesis

As shown in Scheme 2, polyamides **7a**–**h** having adamantylphenoxy-substituted triphenylamino units were synthesized from the diamine monomer **5** with various aromatic dicarboxylic acids **6a**–**h** in NMP containing dissolved calcium chloride by the Yamazaki–Higashi reaction conditions [55] by using TPP and pyridine as condensing agents. All the polycondensation reactions proceeded readily in a homogenous solution, and the reaction solutions generally became very viscous within 1 h. Viscosities of the resultant polymer solutions were normally very high, and the nature of the precipitated polymers (as tough fibrous precipitates) implied high-molecular-weight products. As shown in Table 1, the obtained polyamides **7a–h** had inherent viscosities in the range of 0.39–1.46 dL/g. Except for **7b**, all the **7** series polyamides could be solution-cast into flexible and tough films. The cast film of polymer **7b** was slightly brittle, possibly due to its relatively lower molecular weight. Structural features of these polyamides were verified by FT-IR spectra based on characteristic absorption bands observed around 3300 cm^{-1} (N–H str) and 1652 cm^{-1} (C═O str). Fig. 5a illustrates a typical FTIR spectrum of the representative polyamide **7a**.

Polyimides **10a–f** were prepared in a conventional two-step procedure by the reactions of equal molar amounts of diamine **5** with commercially available aromatic tetracarboxylic dianhydrides (PMDA, BPDA, BTDA, ODPA, DSDA, and 6FDA) in DMAc to form precursor poly(amic acid)s, followed by thermal or chemical cyclodehydration (Scheme 3). As shown in Table 2, the inherent viscosities of the poly(amic acid)s **9a–f** ranged from 1.14 to 1.37 dL/g. The molecular weights of all the poly(amic acid)s were sufficiently high to permit the casting of flexible and tough poly(amic acid) films, which were subsequently converted into tough polyimide films at elevated temperatures. These poly(amic acid)s were also chemically imidized to the corresponding polyimides by treatment of acetic anhydride and pyridine. The chemical structure of the polyimides was confirmed by means of FTIR and NMR spectroscopy. A typical set of IR spectra for poly(amic acid)

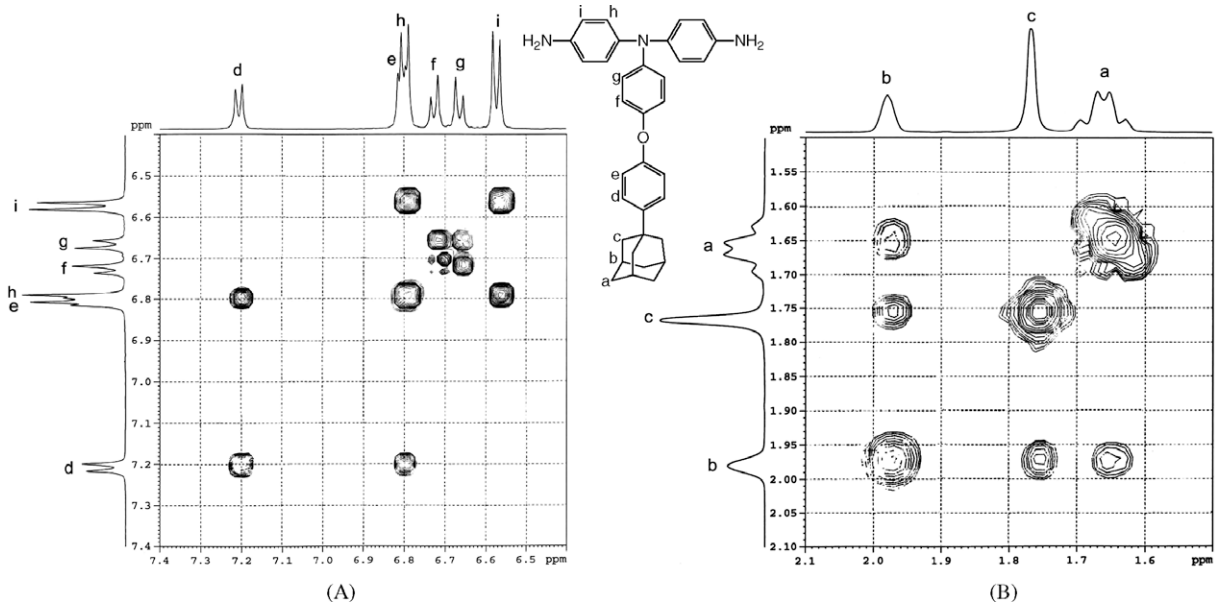

Fig. 3. H–H COSY spectra of diamine monomer **5**: (A) aromatic region and (B) adamantyl group.

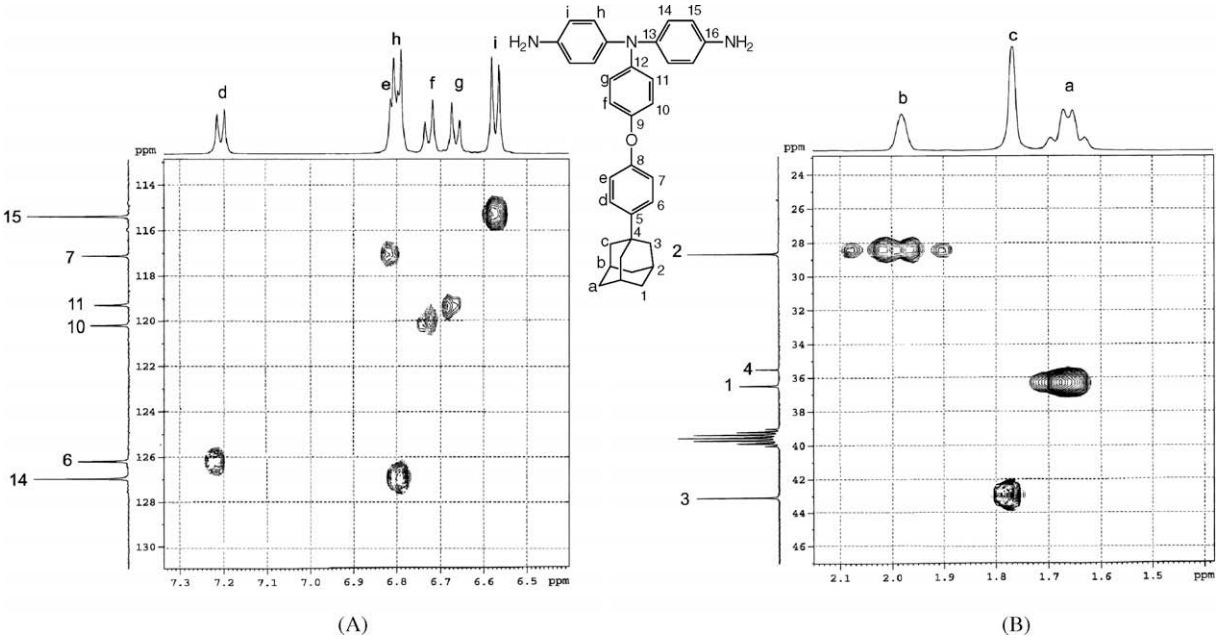

Fig. 4. H–C HETCOR spectra of diamine monomer **5**: (A) aromatic region and (B) adamantyl group.

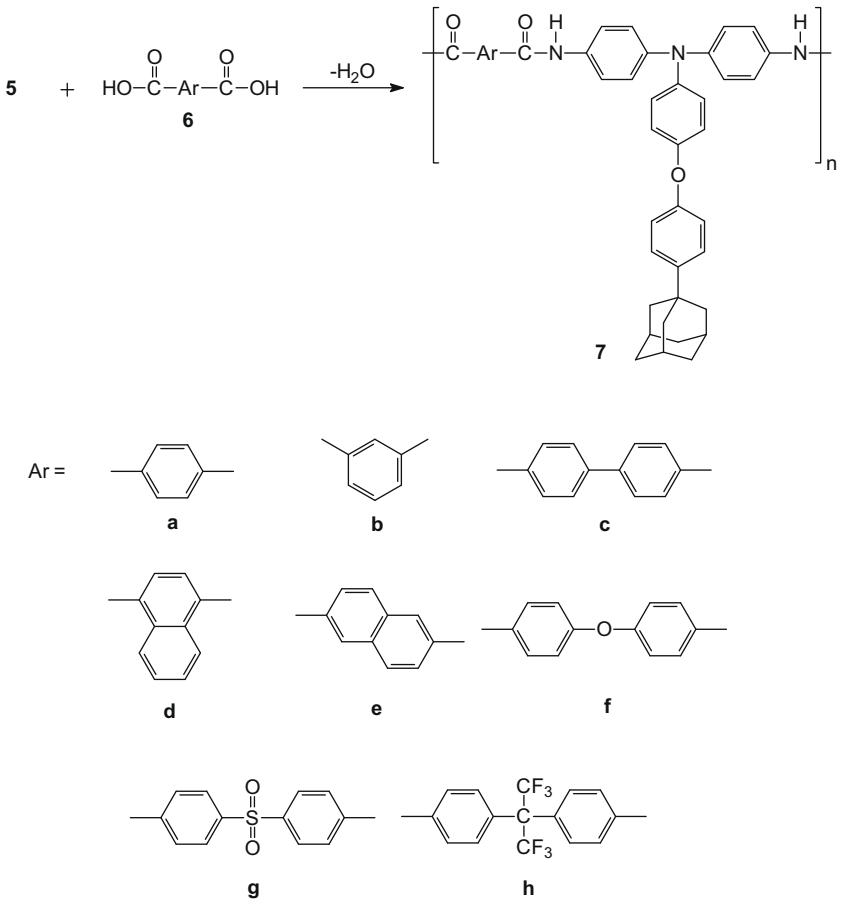

Scheme 2. Synthesis of polyamides.

Table 1
Inherent viscosity and solubility behavior of the polyamides.

Polymer code	η_{inh}[a] (dL/g)	Solubility in various solvents[b]					
		NMP	DMAc	DMF	DMSO	*m*-Cresol	THF
7a	1.46	++	++	++	+	+	–
7b	0.39	++	++	++	+	+	–
7c	1.17	++	++	++	+	+	–
7d	0.64	++	++	++	+	+	–
7e	0.69	++	++	–	+	+	–
7f	0.42	++	++	++	+	+	–
7g	0.73	++	++	++	+	+	–
7h	0.87	++	++	++	+	+	–

The symbol ++: soluble at room temperature; +: soluble on heating at 100 °C or boiling temperature; –: insoluble even on heating.
[a] Inherent viscosity measured at a concentration of 0.5 g/dL in DMAc –5 wt.% LiCl at 30 °C.
[b] Qualitative solubility was determined by using 10 mg sample in 1 mL of stirred solvent. NMP = *N*-methyl-2-pyrrolidone; DMAc = *N*,*N*-dimethylacetamide; DMF = *N*,*N*-dimethylformamide; DMSO = dimethyl sulfoxide; THF = tetrahydrofuran.

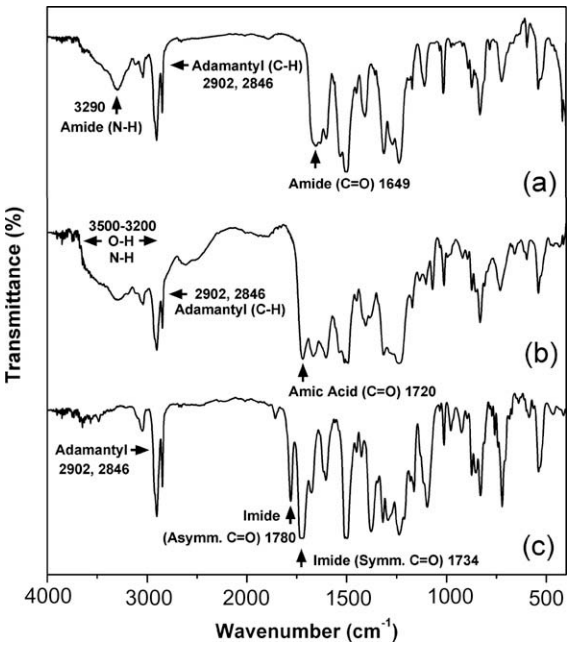

Fig. 5. Thin film IR spectra of (a) polyamide **7a**, (b) poly(amic acid) **9f**, and (c) polyimide **10f**.

9f and its thermally cured polyimide **10f** are also included in Fig. 5. The absorption bands around 1780 and 1720 cm^{-1} arising from the unsymmetrical and symmetrical carbonyl stretching vibrations of the imide groups were found in all the polyimides. There was no existence of the characteristic absorption bands of the amide and carboxyl groups in the region of 3200–3500 cm^{-1} (N–H and O–H stretching), and this indicated that a virtually complete imidization had been obtained. The absorption bands in the range of 2840–2910 cm^{-1} were assigned to methylene and methine C–H stretching of the adamantyl groups. The ^1H NMR spectrum of a representative polyimide **10f** is reproduced in Fig. 6 and agrees well with the desired polymer structure.

3.3. Properties of polymers

3.3.1. Organo-solubility and film property

The solubility properties of polyamides and polyimides in several organic solvents at 10% (w/v) are reported in Tables 1 and 2, respectively. The three-dimensional TPA unit together with the bulky adamantyl-substituted phenoxy pendent group in the repeat units restricted close chain-packing and increased interchain free volume. As a result, these polymers generally revealed an enhanced solubility with respect to conventional aromatic polyamides and polyimides. Almost all the **7** series polyamides were readily soluble in polar solvents such as NMP, DMAc, DMF, DMSO, and *m*-cresol at room temperature or upon heating at 100 °C. For the thermally cured polyimide samples, **10e-H** (from DSDA) and **10f-H** (from 6FDA) showed better solubility than the other polyimides; they could be dissolved in amide-type dipolar solvents, such as NMP, DMAc, and DMF, at room temperature or upon heating. The strong solubilization effect of the sulfonyl groups and hexafluoroisopropylidene groups existing in polyimides **10e** and **10f**, respectively, should contribute to the solubility enhancement. Polyimide **10f** also showed good solubility in less polar solvents like THF because of the additional contribution of the hexafluoroisopropylidene fragment in the polymer backbone. The polyimides prepared by the chemical imidization method showed a higher solubility than those obtained by the thermal imidization method. All the chemically imidized polyimides were soluble in NMP and *m*-cresol at room temperature or elevated temperature. This result indicated that all of these polyimides are organosoluble in nature and can be prepared from the one-step high-temperature polycondensation method. Thus, all the chemically imidized polyimides can be processed from solution. The less solubility of the thermally cured polyimides might be attributable to the better chain-packing and aggregation or partial crosslinking within polymer chains that occurred at elevated temperatures. The good solubility makes these polymers potential candidates for practical applications in spin-coating and inkjet-printing processes. As mentioned earlier, almost all the polymers could afford flexible and tough films. The tensile strengths, elongations to break, and initial moduli

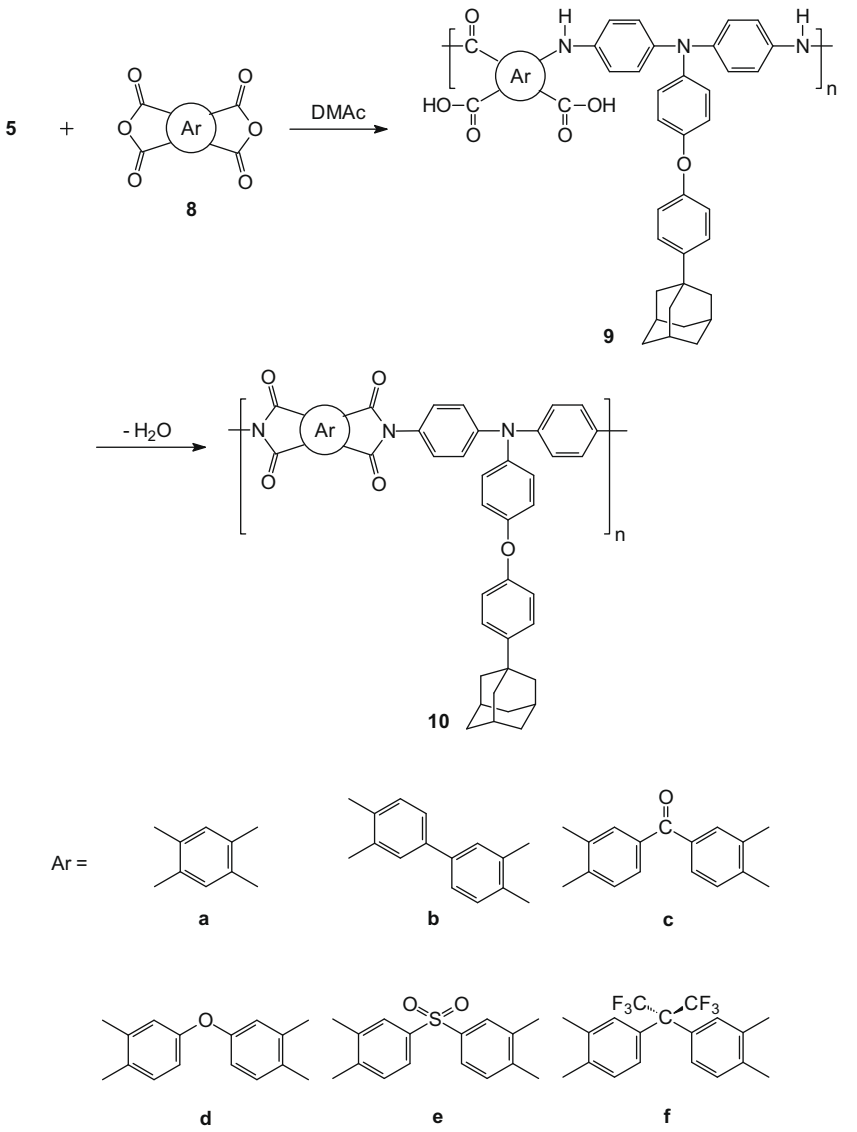

Scheme 3. Synthesis of polyimides.

of these films were in the range of 80–102 MPa, 7–14%, and 2.2–2.6 GPa, respectively, indicative of strong and tough polymeric materials. The WAXD studies of these film samples indicated that all the polymers were essentially amorphous. Their high solubility and amorphous properties can be attributed mainly to the incorporation of bulky, three-dimensional adamantylphenoxy-TPA moiety along the polymer backbone, which results in a high steric hindrance for close packing, and thus reduces their crystallization tendency and interchain interactions.

3.3.2. Thermal properties

DSC, TMA, and TGA were used to evaluate the thermal properties of all polymers. The thermal behavior data of all polyamides and polyimides are summarized in Table 3. The glass-transition temperatures (T_g) of polyamides **7a–7h** could be easily determined in the DSC thermograms; they were observed in the range from 254 °C to 293 °C. The lowest T_g value of polyamide **7f** can be explained in terms of the flexibility and low rotation barrier of its diacid component. The T_gs of polyimides **10a–10f** were observed in the range of 273–310 °C by DSC. As expected, the polyimide **10d** obtained from ODPA showed the lowest T_g of 273 °C due to the presence of a flexible ether linkage between the phthalimide units, and the highest T_g of 310 °C was observed for polyimide **10a** derived from PMDA because of the rigid pyromellitimide segment. All the polymers indicated no clear melting endotherms on their DSC traces, supporting the amorphous nature of these polymers. The softening temperatures (T_s may be referred as apparent T_g) of the polymer films were determined by the TMA method using a loaded penetration probe. They

Table 2
Inherent viscosities and solubility of polyimides.

Code	η_{inh}[a] (dL/g)	Solubility in various solvents[b]					
		NMP	DMAc	DMF	DMSO	*m*-Cresol	THF
10a-C	1.23	++	–	–	–	+	–
10b-C	1.32	+	–	–	–	+	–
10c-C	1.35	++	±	–	++	+	–
10d-C	1.37	++	–	++	–	++	–
10e-C	1.14	++	++	++	++	+	–
10f-C	1.14	++	++	++	++	++	++
10a-H	1.23	–	–	–	–	–	–
10b-H	1.32	–	–	–	–	±	–
10c-H	1.35	–	–	–	–	–	–
10d-H	1.37	–	–	–	–	+	–
10e-H	1.14	++	+	+	–	±	–
10f-H	1.14	++	++	++	–	+	++

10-C: polyimide samples prepared via chemical imidization; **10-H**: samples prepared by heat treatment. The symbol ++: soluble at room temperature; +: soluble on heating at 100 °C or boiling temperature; ±: partially soluble or swelling; –: insoluble even on heating.
[a] Inherent viscosities of the poly(amic acid) precursors measured at a polymer concentration of 0.5 g/dL in DMAc at 30 °C.
[b] The solubility was tested with 10 mg sample in 1 mL of stirred solvent. NMP = *N*-methyl-2-pyrrolidone; DMAc = *N*,*N*-dimethylacetamide; DMF = *N*,*N*-dimethylformamide; DMSO = dimethyl sulfoxide; THF = tetrahydrofuran.

Table 3
Thermal properties of polyamides and polyimides.

Polymer code	T_g[a] (°C)	T_s[b] (°C)	T_d at 5 wt.% loss[c] (°C)		T_d at 10 wt.% loss[c] (°C)		Char yield[d] (%)
			In N_2	In air	In N_2	In air	
7a	273	285	488	491	526	540	58
7b	258	258	477	495	510	539	58
7c	293	282	483	484	527	532	71
7d	268	262	460	449	493	497	60
7e	284	286	471	476	511	528	64
7f	254	254	493	448	530	510	58
7g	286	283	469	468	494	500	56
7h	281	272	479	477	525	519	61
10a	310	305	537	530	558	560	67
10b	296	288	546	550	565	576	59
10c	281	271	532	533	557	561	64
10d	273	270	550	552	567	579	58
10e	293	283	488	485	527	528	52
10f	280	280	535	536	555	562	59

[a] The sample were heated from 50 to 400 °C at a scan rate of 20 °C/min followed by rapid cooling to 50 °C at −200 °C/min in nitrogen. The midpoint temperature of baseline shift on the subsequent DSC trace (from 50 to 400 °C at heating rate 20 °C/min) was defined as T_g.
[b] Softening temperature measured by TMA using a penetration method.
[c] Decomposition temperature at which a 5% or 10% weight loss was recorded by TGA at a heating rate of 20 °C/min.
[d] Residual weight percentages at 800 °C under nitrogen flow.

were read from onset temperature of probe displacement on the TMA trace. As a representative example, the TMA trace of polyimide **10d** is illustrated in Fig. 7. As listed in Table 3, the T_s values of the **7** series polyamides and the **10** series polyimides were in the range of 254–286 °C and 270–305 °C, respectively. The trend of T_s variation with the chain stiffness was similar to that of T_g observed in the DSC measurements.

The thermal stability of the polymers was evaluated by TGA measurements in both air and nitrogen atmospheres. Typical TGA curves for polyamide **7a** and polyimide **10a** are reproduced in Fig. 8. These polymers exhibited reasonable thermal stability without significant weight loss up to 450 °C (for the polyamides) or 500 °C (for the polyimides) under nitrogen or air atmosphere. The decomposition temperatures (T_d) at 5% and 10% weight loss in nitrogen and in air atmospheres were determined from the original TGA thermograms and are also given in Table 3. The T_d at 10% weight loss of polyamides **7a–7h** in nitrogen and in air stayed in the range of 493–530 °C and 497–540 °C, respectively, and those for polyimides **10a–10f** were recorded in the range of 485–552 °C and 528–579 °C, respectively. All the polymers left more than 52% char yield at 800 °C in nitrogen. Thus, the TGA data indicated that these polymers had fairly high thermal stability even with the introduction of bulky adamantyl pendent groups.

3.3.3. Optical and electrochemical properties

The optical properties of these polymers were investigated by UV–vis and photoluminescence (PL)

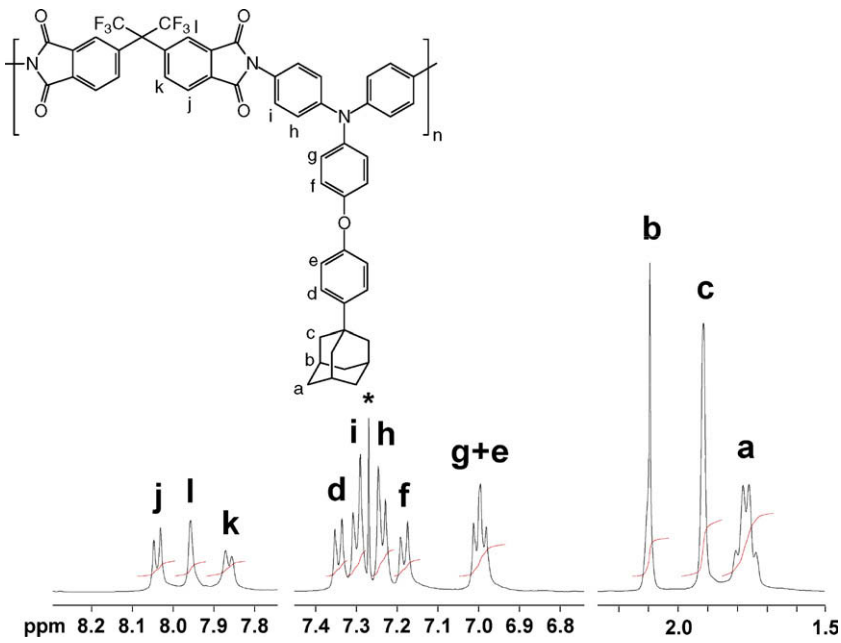

Fig. 6. ^{1}H NMR spectrum of polyimide **10f** in $CDCl_3$ (∗ the solvent peak).

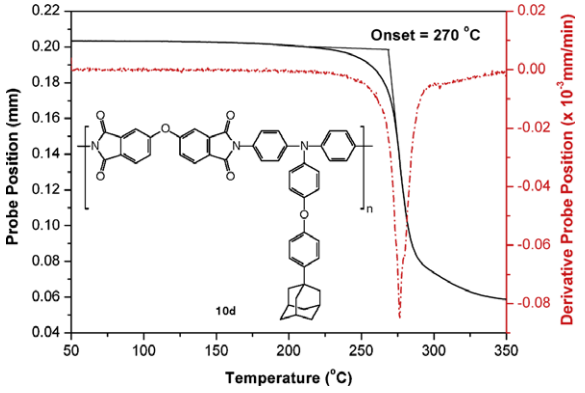

Fig. 7. TMA curve of polyimide **10d** with a heating rate of 10 °C/min.

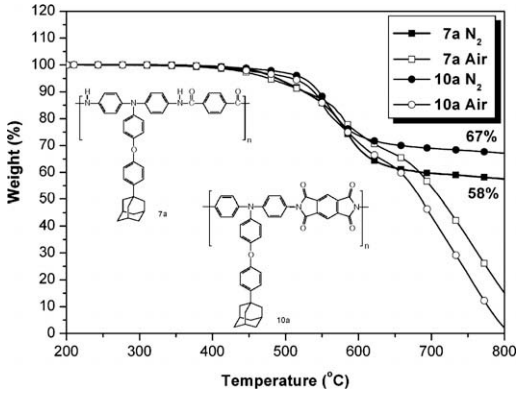

Fig. 8. TGA thermograms of polyamide **7a** and polyimide **10a** at a scan rate of 20 °C/min.

spectroscopy. The absorption λ_{max} and λ_{onset} (absorption edge) and PL λ_{max} data are reported in Table 4. The polyamides exhibited strong UV–vis absorption bands at 293–346 nm in dilute NMP solutions (10^{-5} M), assignable to the π–π^* transition resulting from the TPA moieties. Their PL spectra in NMP solution showed emission peaks around 408–452 nm in the blue region. Typical UV–vis absorption and PL spectra together with the PL images of some polyamide solutions are illustrated in Fig. 9. Optical band gap (E_g^{opt}) determined from the λ_{onset} values of the solid-state absorption spectra of the polyamides were found to be 2.62–3.01 eV. The polyimides present similar spectra in dilute NMP solutions and in the solid state, with λ_{max} at 302–322 nm. They exhibited significantly less detectable fluorescence than the polyamides. We propose that the observed quenching of PL that occurs in the polyimides is due to re-absorption by the charge transfer complexing between the donor triphenylamine and acceptor imide units.

The redox behavior was monitored by cyclic voltammetry (CV) conducted for the cast film on an ITO-coated glass substrate as working electrode in dry acetonitrile (CH_3CN) containing 0.1 M of TBAP as an electrolyte under nitrogen atmosphere. A pair of reversible redox couple could be observed on the CV scans of all polymers. Typical CV curves for polyamide **7h** and polyimide **10f** are shown in Fig. 10, and the half-wave potentials ($E_{1/2}$; average potential of the redox couple peaks) of all polyamides and polyimides are also summarized in Table 4. The polyamides exhibited $E_{1/2}$ values in the range of 0.83–0.86 V, corresponding to TPA oxidation. The color of the polyamide films changed from colorless or light yellow to green because of electrochemical oxidation of the polymers. The oxidative and electrochromic reversibility is maintained on repeated

Table 4
Optical and electrochemical properties of the polyamides and polyimides.

Code	Abs λ_{max}[a] (nm)	Abs λ_{onset}[a] (nm)	PL λ_{max}[b] (nm)	$E_{1/2}$[c] (V) (vs. Ag/AgCl)	E_g^{opt}[d] (eV)	HOMO/LUMO[e] (eV)
7a	293 (363)	425 (456)	440	0.84	2.72	5.16/2.44
7b	338 (342)	395 (430)	417	0.84	2.88	5.16/2.28
7c	298 (362)	421 (440)	449	0.83	2.82	5.15/2.33
7d	314 (342)	399 (411)	408	0.84	3.01	5.16/2.15
7e	301 (362)	438 (472)	452	0.83	2.63	5.15/2.52
7f	336 (351)	390 (423)	416	0.84	2.93	5.16/2.23
7g	300 (319)	457 (474)	449	0.85	2.62	5.17/2.55
7h	346 (358)	408 (460)	418	0.86	2.70	5.18/2.48
10a	308 (315)	396 (426)	474	1.13	2.91	5.45/2.54
10b	322 (325)	366 (397)	475	1.12	3.12	5.44/2.32
10c	306 (313)	375 (399)	479	1.12	3.11	5.44/2.33
10d	315 (319)	360 (389)	440	1.12	3.19	5.44/2.25
10e	302 (311)	379 (403)	480	1.12	3.08	5.44/2.36
10f	306 (329)	373 (389)	472	1.12	3.19	5.44/2.25

[a] UV–vis absorption measurements in NMP (10^{-5} M) at room temperature, values in parentheses are polymer thin solid-film.
[b] PL spectra measurements in NMP (10^{-5} M) at room temperature.
[c] Oxidation half-wave potentials from cyclic voltammograms.
[d] Optical energy gap = $1240/\lambda_{abs,\ onset}$ of polymer thin film.
[e] The HOMO energy levels were calculated from $E_{1/2}$ and were referenced to ferrocene (4.8 eV); LUMO = HOMO − E_g^{opt}.

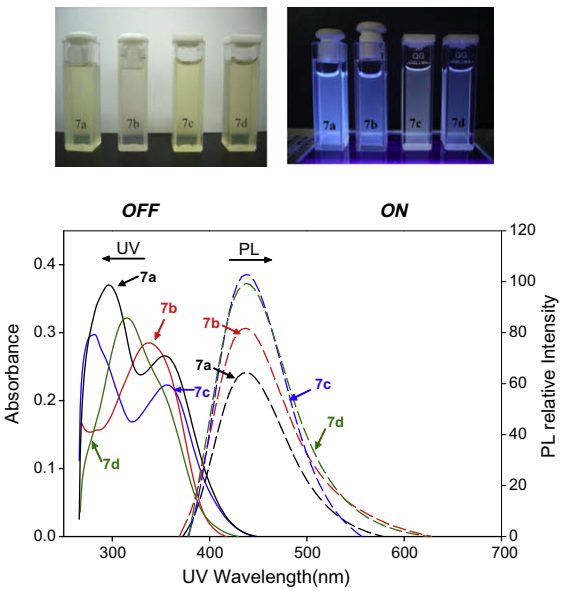

Fig. 9. UV–vis absorption and PL spectra of polyamides **7a**–**7d** with a concentration of 10^{-5} M in NMP. The photographs show their images before and when illuminated with a standard laboratory UV lamp.

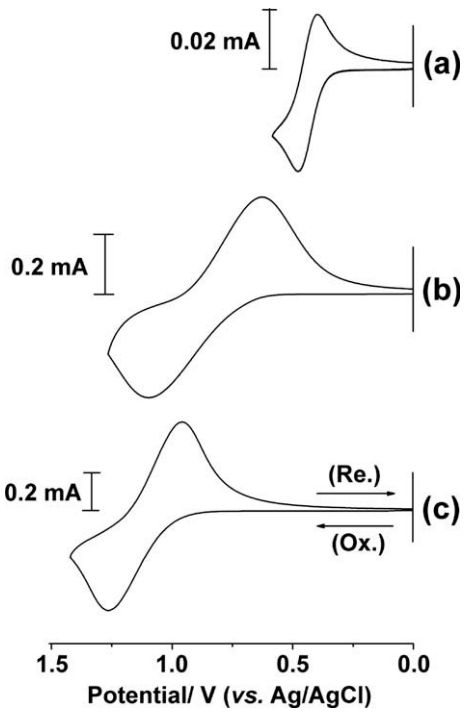

Fig. 10. Cyclic voltammograms of (a) ferrocene, (b) the cast film of polyamide **7h**, and (c) polyimide **10f** on an indium–tin oxide (ITO)-coated glass substrate at a scan rate of 100 mV/s in 0.1 M TBAP/acetonitrile.

scanning between 0 V and 1.1 V (vs. Ag/AgCl). This result confirms that *para*-substitution of the adamantylphenoxy group on the TPA unit leads considerable stability to the radical cation species. The oxidation of polyimides started to occur at higher potentials than the polyamides because of the electron-withdrawing effect arising from the imide group. Their $E_{1/2}$ values were recorded in the 1.12–1.13 V range. The color of the polyimide films turned from pale yellow to blue upon oxidation. However, the polyimide samples revealed a less redox stability with respect to the polyamide ones. They generally lost redox and electrochromic reversibility after some tens of repeated CV scans.

The $E_{1/2}$ value of ferrocene/ferrocenium (Fc/Fc^+) is known to be 4.8 eV below the vacuum level and was used as a calibration reference. The highest occupied molecular orbital (HOMO) energy levels of the **7** series polyamides and the **10** series polyimides estimated from their $E_{1/2}$ values were in the range of 5.15–5.18 eV and 5.44–5.45 eV, respectively; these HOMO levels were comparable to those of small hole-transporting molecules [1,2]. It can be

concluded that these novel adamantylphenoxy-TPA polymers which are soluble in common solvents and which possess good film-forming properties turn out to be good hole-transport materials with improved stability as compared to the low molecular weight compounds.

3.3.4. Spectroelectrochemical and electrochromic properties

Spectroelectrochemical analysis of the polyamide and polyimide thin films was carried out on an ITO-coated glass substrate in an acetonitrile solution of 0.1 M TBAP by applying the desired potential. All the polymer films showed a strong coloration change when the applied potential was changed. The typical changes of the absorption spectra of polyamide **7h** are shown in Fig. 11. When the applied potential increased from 0.80 to 1.10 V, the peak of characteristic absorbance at 346 nm for polyamide **7h** decreased gradually while new band grew up at 785 nm, and the color of the film changed to green. The spectral changes were clearly due to the formation of the cationic states of polyamide **7h**.

The typical absorption spectral change of polyimide **10f** is depicted in Fig. 12. When the applied potential was in the 0–1.0 V range, the absorption bands of the polyimide films did not change remarkedly. As the applied potential was increased to 1.05 V, the absorbance intensity at 306 nm decreased, and a new absorption band appeared at about 755 nm. On application of a higher positive potential of 1.3 or 1.4 V, another new absorption peak appeared at about 379 nm and the intensity of the absorption band at 755 nm increased in intensity, and the color of the film changed to blue (as shown in Fig. 12). The new spectrum was assigned as that of the formation of a cationic radical species of the polyimide **10f**. However, the long-term electrochromic stability of all the polyimides was lower than the polyamides because of the relatively lower stability of their cationic radical species.

The stability and response time upon electrochromic switching of the cast film of polyamide **7h** between its neutral and oxidized forms in the UV–vis region was monitored. The switching time of color was estimated by applying a potential step, and the absorbance profiles were followed (Fig. 13). The switching time was calculated at 90% of the full switch because it is difficult to perceive any further color change with naked eye beyond this point. Thin films from polyamide **7h** would require 3.3 s at 1.10 V for coloring and 2.4 s for bleaching. After hundreds of switching at voltage between 0 V and 1.1 V, the polymer films still exhibited excellent stability of electrochromic characteristics. However, as we can see in Fig. 14, after continuous 10 cyclic scans between 0 V and 1.4 V, the thin film of polyimide **10f** exhibited a decreased optical switching reversibility. The less stability might be attributable to the electron-withdrawing effect of the imide group.

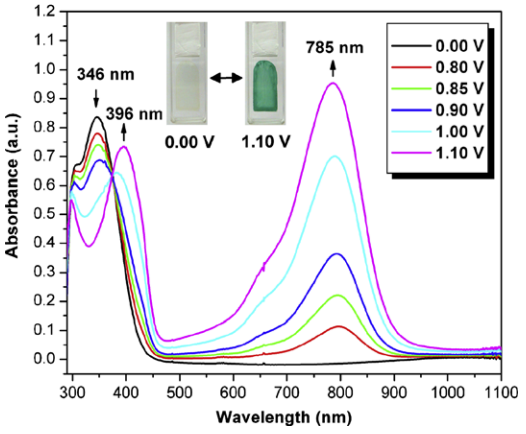

Fig. 11. Spectral change of polyamide **7h** thin film on the ITO-coated glass substrate (in CH_3CN with 0.1 M TBAP as the supporting electrolyte) along with increasing of the applied voltage (vs. Ag/AgCl couple as reference). The inset shows the photographic images of the film at indicated applied voltages.

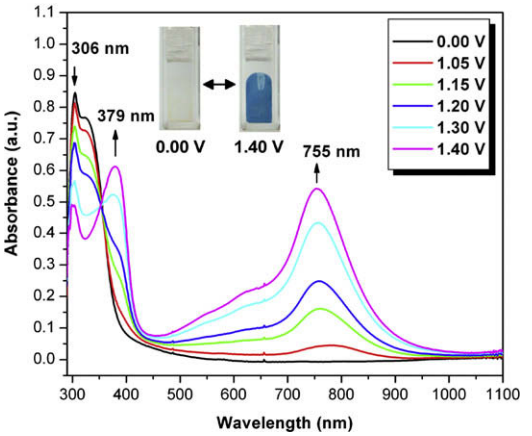

Fig. 12. Spectral change of polyimide **10f** thin film on the ITO-coated glass substrate (in CH_3CN with 0.1 M TBAP as the supporting electrolyte) along with increasing of the applied voltage (vs. Ag/AgCl couple as reference). The inset shows the photographic images of the film at indicated applied voltages.

4. Conclusions

The novel triphenylamine-based diamine monomer, 4-[4-(1-adamantyl)phenoxy]-4′,4″-diaminotriphenylamine

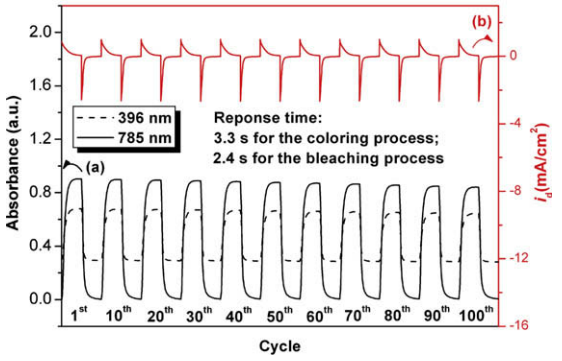

Fig. 13. (a) Potential step absorptometry and (b) kinetically current consumption of polyamide **7h** film onto the ITO-coated glass substrate during the continuous cycling test by switching potentials between 0 V and 1.10 V (vs. Ag/AgCl) with a cycle time of 22 s.

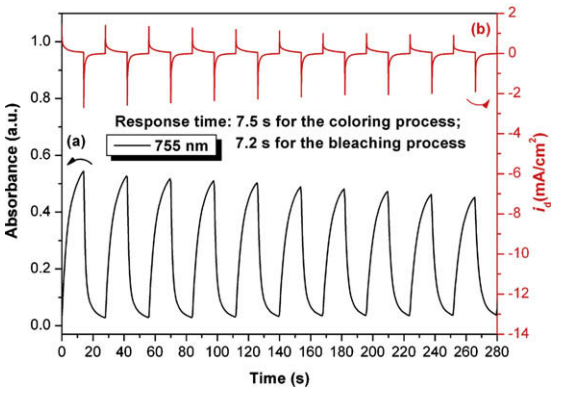

Fig. 14. (a) Potential step absorptometry and (b) kinetically current consumption of polyimide **10f** film onto the ITO-coated glass substrate during the continuous cycling test by switching potentials between 0 V and 1.40 V (vs. Ag/AgCl) with a cycle time of 28 s.

has been successfully synthesized in this study. Two series of electroactive aromatic polyamides and polyimides with adamantyl-substituted phenoxy pendent groups were synthesized from the polycondensation reactions of this newly synthesized diamine monomer with various aromatic dicarboxylic acids and tetracarboxylic dianhydrides, respectively. The three-dimensional triphenylamino group can disrupt the coplanarity of aromatic units in chain packing, and the bulky adamantly pendent group increases the between-chains spaces or free volume; consequently, all the polymers were amorphous with good solubility in many polar solvents and exhibited excellent film-forming ability. In addition to high glass transition temperature, high thermal stability, and good mechanical properties, these polymers especially for the polyamides also revealed excellent stability of electrochromic characteristics. As a result, the present polyamides and polyimides may find applications as new type high-temperature hole-transporting polymeric materials and organic electrochromics.

Acknowledgment

The authors are grateful to the *National Science Council* of the *Republic of China* for financial support of this work.

References

[1] Shirota Y. J Mater Chem 2000;10:1.
[2] Shirota Y. J Mater Chem 2005;15:75.
[3] Thelakkat M. Macromol Mater Eng 2002;287:442.
[4] Liu Y, Liu MS, Li XC, Jen AKY. Chem Mater 1998;10:3301.
[5] Li XC, Liu Y, Liu MS, Jen AKY. Chem Mater 1999;11:1568.
[6] Redecker M, Bradley DDC, Inbasekaran M, Wu WW, Woo EP. Adv Mater 1999;11:241.
[7] Miteva T, Meisel A, Knoll W, Nothofer HG, Scherf U, Muller DC, et al. Adv Mater 2001;13:565.
[8] Pu YJ, Soma M, Kido J, Nishide H. Chem Mater 2001;13:3817.
[9] Ego C, Grimsdale AC, Uckert F, Yu G, Srdanov G, Mullen K. Adv Mater 2002;14:809.
[10] Shu CF, Dodda R, Wu FI, Liu MS, Jen AKY. Macromolecules 2003;36:6698.
[11] Liang F, Pu YJ, Kurata T, Kido J, Nishide H. Polymer 2005;46:3767.
[12] Kim YH, Zhao Q, Kwon SK. J Polym Sci Part A Polym Chem 2006;44:172.
[13] Yang HH. Aromatic high-strength fibers. New York: Wiley; 1989.
[14] Wilson D, Stenzenberger HD, Hergenrother PM, editors. Polyimides. London: Blackie; 1990.
[15] Sroog CE. Prog Polym Sci 1991;16:561.
[16] Ghosh MM, Mittal KL, editors. Polyimides: fundamentals and applications. New York: Marcel Dekker; 1996.
[17] Imai Y. High Perform Polym 1995;7:337.
[18] Imai Y. React Funct Polym 1996;30:3.
[19] Huang SJ, Hoyt AE. Trends Polym Sci 1995;3:262.
[20] De Abajo J, De la Campa JG. Adv Polym Sci 1999;140:23.
[21] Eastmond GC, Gibas M, Paprotny J. Eur Polym J 1999;35:2097.
[22] Wu SC, Shu CF. J Polym Sci Part A Polym Chem 2003;41:1160.
[23] Myung BY, Kim JS, Kim JJ, Yoon TH. J Polym Sci Part A Polym Chem 2003;41:3361.
[24] Hsiao SH, Chang YH. J Polym Sci Part A Polym Chem 2004;42:1225.
[25] Hsiao SH, Chang YM. J Polym Sci Part A Polym Chem 2004;42:4056.
[26] Lin CH, Lin CH. J Polym Sci Part A Polym Chem 2007;45:2897.
[27] Zhang Q, Li S, Li W, Zhang S. Polymer 2007;48:6246.
[28] Wang CY, Li G, Jiang JM. Polymer 2009;50:1709.
[29] Oishi Y, Takado H, Yoneyama M, Kakimoto M, Imai Y. J Polym Sci Part A Polym Chem 1990;28:763.
[30] Oishi Y, Ishida M, Kakimoto M, Imai Y, Kurosaki T. J Polym Sci Part A Polym Chem 1992;30:1027.
[31] Liou GS, Hsiao SH, Ishida M, Kakimoto M, Imai Y. J Polym Sci Part A Polym Chem 2002;40:810.
[32] Liou GS, Hsiao SH, Ishida M, Kakimoto M, Imai Y. J Polym Sci Part A Polym Chem 2002;40:3815.
[33] Liaw DJ, Hsu PN, Chen WH, Lin SL. Macromolecules 2002;35:4669.
[34] Liou GS, Hsiao SH. J Polym Sci Part A Polym Chem 2003;41:94.
[35] Hsiao SH, Chen CW, Liou GS. J Polym Sci Part A Polym Chem 2004;42:3302.
[36] Li W, Li S, Zhang Q, Zhang S. Macromolecules 2007;40:8205.
[37] Cheng SH, Hsiao SH, Su TH, Liou GS. Macromolecules 2005;38:307.
[38] Su TH, Hsiao SH, Liou GS. J Polym Sci Part A Polym Chem 2005;43:2085.
[39] Liou GS, Hsiao SH, Su TH. J Mater Chem 2005;15:1812.
[40] Hsiao SH, Chang YM, Chen HW, Liou GS. J Polym Sci Part A Polym Chem 2006;44:4579.
[41] Chang CW, Liou GS, Hsiao SH. J Mater Chem 2007;17:1007.
[42] Liou GS, Chang CW. Macromolecules 2008;41:1667.
[43] Hsiao SH, Liou GS, Kung YC, Yen HJ. Macromolecules 2008;41:2800.
[44] Fort Jr RC, Schleyer PvR. Chem Rev 1964;64:277.
[45] Chern YT, Chung WH. J Polym Sci Part A Polym Chem 1996;34:117.
[46] Chern YT, Shiue HC. Macromolecules 1997;30:4646.
[47] Chern YT, Lin KS, Kao SC. J Appl Polym Sci 1998;68:315.
[48] Chern YT, Shiue HC, Kao SC. J Polym Sci Part A Polym Chem 1998;36:785.
[49] Chern YT, Shiue HC. Macromol Chem Phys 1998;199:963.
[50] Hsiao SH, Li CT. Macromolecules 1998;31:7213.
[51] Hsiao SH, Li CT. J Polym Sci Part A Polym Chem 1999;37:1435.
[52] Kwak SM, Yeon JH, Yoon TH. J Polym Sci Part A Polym Chem 2006;44:2567.
[53] Kung YC, Liou GS, Hsiao SH. J Polym Sci Part A Polym Chem 2009;47:1740.
[54] Jensen JJ, Grimsley M, Mathias LJ. J Polym Sci Part A Polym Chem 1996;34:397.
[55] Yamazaki N, Matsumoto M, Higashi F. J Polym Sci Polym Chem Ed 1975;13:1373.